

# Mobile Speed Estimation Based on Average Fade Slope Duration

Lian Zhao, *Member, IEEE*, and Jon W. Mark, *Life Fellow, IEEE*

**Abstract**—Based on the zero crossing rate of the slope (first derivative) of the underlying fading process, a mobile speed-estimation scheme, constructed by counting the average number of sampling steps in a positive-going (and/or negative-going) fade envelope slope, is proposed. The proposed speed-estimation approach requires neither knowledge of the average fade power nor a variable temporal observation window. The computational complexity and the required memory storage are negligibly small. Simulation results show that the proposed speed estimator yields good estimation accuracy, with relatively small estimation error.

**Index Terms**—Average fade slope duration (AFSD), envelope slope zero crossing rate (ZCR), histogram, sampling, speed estimation.

## I. INTRODUCTION

KNOWLEDGE of the mobile speed or Doppler frequency is invaluable to radio resource management. The ability to accurately estimate the mobile speed is very important. The envelope function of the fade contains rich information for speed estimation. Examples of speed-estimation approaches using fading envelope information include level crossing rate (LCR) [1], autocovariance of the complex envelope [1]–[3], squared deviation of the logarithmically compressed signal envelope [2], and mean distance between the local minima using continuous wavelet transform (CWT) [4].

It is well known that the LCR of a fading process is related to Doppler frequency and average fading power. In this letter, we will show that higher order crossing is only related to Doppler frequency. We will first derive the zero crossing rate (ZCR) of the slope of the underlying fading process in terms of its characteristic function (CF). Compared to the method in [4], our approach avoids the integration over the modified Bessel function of the first kind of order  $\pm 1/4$ . Using the ZCR result, we propose a speed-estimation scheme based on counting the average number of sampling intervals in a positive-going (and/or negative-going) slope of the fade envelope. For this purpose, we introduce a new parameter called *average fade slope duration* (AFSD), which is defined as the average number of sampling steps during an interval when the envelope transits from a minimum to a maximum, or from a maximum to a minimum.

Paper approved by I. Lee, the Editor for Wireless Communication Theory of the IEEE Communications Society. Manuscript received August 20, 2003; revised March 12, 2004. This work was supported by the Natural Sciences and Engineering Research Council (NSERC) of Canada under Grants RGPIN7779 and 293237-04.

L. Zhao was with the Centre for Wireless Communications, Electrical and Computer Engineering Department, University of Waterloo, Waterloo, ON N2L 3G1, Canada. She is now with Ryerson University, Toronto, ON M5B 2K3, Canada.

J. W. Mark is with the Centre for Wireless Communications, Electrical and Computer Engineering Department, University of Waterloo, Waterloo, ON N2L 3G1, Canada (e-mail: jwmark@waterloo.ca).

Digital Object Identifier 10.1109/TCOMM.2004.836591

The proposed estimation scheme is based on observations of the AFSD. As in [4], the proposed approach does not require knowledge of the average fading power, nor a need to make the temporal observation window adaptive. Since the main arithmetical operations are comparisons, the computations required by the estimation algorithm are relatively simple.

Simulation results show that the proposed AFSD-based mobile speed-estimation scheme exhibits good estimation accuracy, with relatively small estimation error. The proposed scheme can process the data and the sampling process concurrently. It only requires a small number of samples and only needs to save the two most recent sample values to complete the estimation.

## II. SYSTEM MODEL

The fast Rayleigh fading process,  $z(t)$ , is modeled using Jakes' fading model [5] and is represented by

$$z(t) = R(t)e^{-j\theta(t)} = U(t) + jV(t) \quad (1)$$

where  $\theta(t)$  is a random phase uniformly distributed on  $[0, 2\pi)$  and  $R(t)$  is a Rayleigh distributed random process, independent of  $\theta(t)$ .  $U(t)$  and  $V(t)$  are independent Gaussian low-pass processes with zero mean and variance  $\sigma^2$ , given by

$$2\sigma^2 = 2E\{U^2(t)\} = 2E\{V^2(t)\} = E\{R^2(t)\} \quad (2)$$

and power spectral density

$$S_U(f) = S_V(f) = \begin{cases} \frac{\sigma^2}{\pi\sqrt{f_d^2 - f^2}}, & |f| \leq f_d \\ 0, & |f| > f_d \end{cases} \quad (3)$$

where  $f_d = v/\lambda$  is the maximum Doppler frequency and  $v$  and  $\lambda$  are, respectively, the mobile speed and wavelength. The envelope process  $R(t)$  follows the Rayleigh probability density function (pdf) given by

$$f_R(x) = \frac{x}{\sigma^2} \exp\left(-\frac{x^2}{2\sigma^2}\right) x > 0. \quad (4)$$

Let  $\dot{R}(t)$  be the first derivative (slope) of  $R(t)$ , the fading envelope, at time instant  $t$ . Assume that the diffuse component of the received bandpass signal is symmetrical about the carrier frequency. The pdf of  $\dot{R}$  follows a Gaussian distribution with zero mean and variance  $\sigma_s^2 = 2(\pi f_d \sigma)^2$  [5]

$$f(\dot{R}) = \frac{1}{\sqrt{2\pi}\sigma_s} \exp\left(-\frac{\dot{R}^2}{2\sigma_s^2}\right). \quad (5)$$

## III. SPEED ESTIMATION USING AFSD

The presence of Doppler frequency (or mobile speed) incurs variations in the fading envelope. We introduce the AFSD, denoted by  $L$ , as a parameter to measure the variations in the fading envelope. AFSD is defined as the average number of

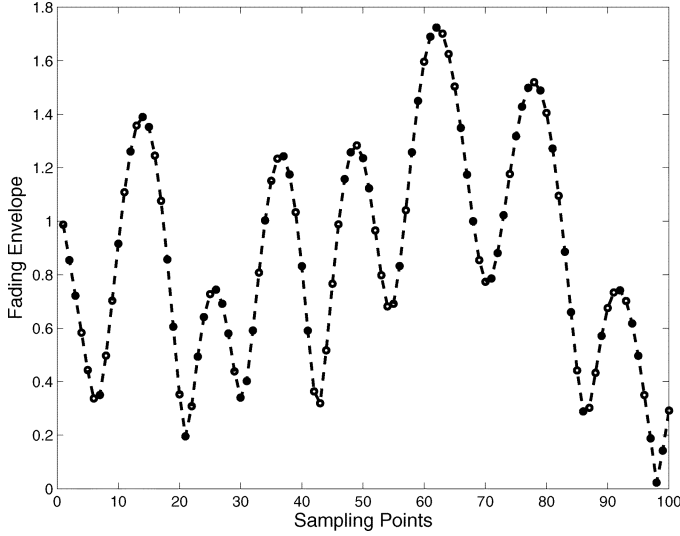


Fig. 1. Typical Rayleigh fading trace.

sampling intervals within a positive or negative fading envelope slope. It turns out that AFSD is independent of the average fading power, but is uniquely determined by the maximum Doppler frequency,  $f_d$ , and the sampling interval  $\tau$ . The proposed speed-estimation method makes use of the observations of  $L$ , and applies the derived relationship between  $L$  and  $f_d$  to estimate  $f_d$ , or equivalently, the mobile speed  $v$ .

Fig. 1 shows a typical fading signal trace as a function of time, with an envelope function alternating between minima and maxima. For the derivation of AFSD, we assume that the positive and negative slopes are statically symmetric, and focus attention on positive-going slopes only.

Since the first derivative of the fading envelope at an extremal point is zero, we can deduce that

$$2L\tau = \frac{1}{ZCR_{\dot{R}}} \quad (6)$$

where  $\tau$  is the sampling interval and  $ZCR_{\dot{R}}$  is the ZCR of  $\dot{R}$ ; its reciprocal is the average time length between adjacent maxima.

Let  $r = R^2$  be the square of the amplitude. Since  $\dot{r} = 2R\dot{R}$ , for a random process, we have  $ZCR_{\dot{r}} = ZCR_{\dot{R}}$ , and we can calculate  $ZCR_{\dot{r}}$  via  $ZCR_{\dot{R}}$  [6], [7]

$$ZCR_{\dot{r}} = \int_{-\infty}^{\infty} |\ddot{r}| f(\dot{r} = 0, \ddot{r}) d\ddot{r} \quad (7)$$

where  $\ddot{r}$  is the second derivative of  $r$ , and  $f(\dot{r}, \ddot{r})$  is the joint pdf of  $\dot{r}$  and  $\ddot{r}$ .

Using the generalized Parseval's theorem for the right-hand side of (7) and invoking the Fourier transform properties, we get [7]

$$\begin{aligned} ZCR_{\dot{r}} &= \frac{-1}{2\pi^2} \int_{-\infty}^{\infty} \int_{-\infty}^{\infty} \frac{1}{\omega_2} \frac{d\Phi_{\dot{r}\ddot{r}}(\omega_1, \omega_2)}{d\omega_2} d\omega_1 d\omega_2 \\ &= \frac{-1}{2\pi^2} \int_{-\infty}^{\infty} \int_{-\infty}^{\infty} \frac{\Phi_{\dot{r}\ddot{r}}(\omega_1, \omega_2) - \Phi_{\dot{r}}(\omega_1)}{\omega_2^2} d\omega_1 d\omega_2 \quad (8) \end{aligned}$$

where  $\Phi_{\dot{r}}$  and  $\Phi_{\dot{r}\ddot{r}}$  are, respectively, the one-dimensional (1-D) and two-dimensional (2-D) CFs.

We start with the three-dimensional CF,  $\Phi_{\dot{r}\ddot{r}}(\omega_0, \omega_1, \omega_2)$ , and then obtain the 2-D and 1-D CFs by setting  $\omega_0 = 0$ , and  $\omega_0 = \omega_1 = 0$ , respectively

$$\begin{aligned} \Phi_{\dot{r}\ddot{r}}(\omega_0, \omega_1, \omega_2) &= E[\exp(j\omega_0 r + j\omega_1 \dot{r} + j\omega_2 \ddot{r})] \\ &= E[\exp(j\omega_0(U^2 + V^2) + 2j\omega_1(U\dot{U} + V\dot{V}) \\ &\quad + 2j\omega_2(\dot{U}^2 + \dot{V}^2 + U\ddot{U} + V\ddot{V}))]. \quad (9) \end{aligned}$$

Let us define the vectors  $\mathbf{W} = [U, V, \dot{U}, \dot{V}, \ddot{U}, \ddot{V}]^T$ . Since differentiation is a linear operation, the processes  $\dot{U}$ ,  $\dot{V}$ ,  $\ddot{U}$ , and  $\ddot{V}$  are also Gaussian. Therefore,  $\mathbf{W}$  is a zero-mean Gaussian vector with covariance matrix

$$\Sigma = \begin{bmatrix} b_0 & 0 & 0 & 0 & -b_2 & 0 \\ 0 & b_0 & 0 & 0 & 0 & -b_2 \\ 0 & 0 & b_2 & 0 & 0 & 0 \\ 0 & 0 & 0 & b_2 & 0 & 0 \\ -b_2 & 0 & 0 & 0 & b_4 & 0 \\ 0 & -b_2 & 0 & 0 & 0 & b_4 \end{bmatrix} \quad (10)$$

where  $b_0 \equiv \sigma^2$ ,  $b_2 = (b_0/2)(2\pi f_d)^2$  and  $b_4 = (3b_0/8)(2\pi f_d)^4$  [6]. Further define

$$\Xi = \begin{bmatrix} \omega_0 & 0 & \omega_1 & 0 & \omega_2 & 0 \\ 0 & \omega_0 & 0 & \omega_1 & 0 & \omega_2 \\ \omega_1 & 0 & 2\omega_2 & 0 & 0 & 0 \\ 0 & \omega_1 & 0 & 2\omega_2 & 0 & 0 \\ \omega_2 & 0 & 0 & 0 & 0 & 0 \\ 0 & \omega_2 & 0 & 0 & 0 & 0 \end{bmatrix}. \quad (11)$$

Then the 3-D CF in (9) can be written as

$$\Phi_{\dot{r}\ddot{r}}(\omega_0, \omega_1, \omega_2) = E[\exp(j\mathbf{W}^T \Xi \mathbf{W})]. \quad (12)$$

The scalar random variable,  $\mathbf{W}^T \Xi \mathbf{W}$ , is a quadratic form of Gaussian random variables, and its CF  $E\{\exp[j\omega(\mathbf{W}^T \Xi \mathbf{W})]\}$  can be evaluated as [7], [8]

$$\begin{aligned} E\{\exp[j\omega(\mathbf{W}^T \Xi \mathbf{W})]\} &= \frac{\exp(-\frac{1}{2}\boldsymbol{\mu}^T \boldsymbol{\Sigma}^{-1} [\mathbf{I} - (\mathbf{I} - 2j\omega \boldsymbol{\Sigma} \Xi)^{-1}] \boldsymbol{\mu})}{\sqrt{\det(\mathbf{I} - 2j\omega \boldsymbol{\Sigma} \Xi)}} \quad (13) \end{aligned}$$

where  $\mathbf{I}$  is a  $6 \times 6$  identity matrix,  $\boldsymbol{\mu}$  is the mean of the Gaussian vector  $\mathbf{W}$ , and  $\det(\cdot)$  denotes the determinant of its argument. Then (12) can be evaluated by replacing  $\omega$  with 1 in (13). After some algebraic manipulation, we obtain

$$\begin{aligned} \Phi_{\dot{r}\ddot{r}}(\omega_0, \omega_1, \omega_2) &= (1 - 8b_0 b_2 \omega_0 \omega_2 + 4b_0 b_2 \omega_1^2 \\ &\quad + 18b_2^2 \omega_2^2 - 2j b_0 \omega_0 - 8j b_2^3 \omega_2^3)^{-1}. \quad (14) \end{aligned}$$

Now the 2-D and 1-D CFs can be obtained as

$$\begin{aligned} \Phi_{\dot{r}\ddot{r}}(\omega_1, \omega_2) &= \Phi_{\dot{r}\ddot{r}}(\omega_0, \omega_1, \omega_2)|_{\omega_0=0} \\ &= \frac{1}{1 + 4b_0 b_2 \omega_1^2 + 18b_2^2 \omega_2^2 - 8j b_2^3 \omega_2^3} \quad (15) \\ \Phi_{\dot{r}}(\omega_1) &= \Phi_{\dot{r}\ddot{r}}(\omega_0, \omega_1, \omega_2)|_{\omega_0=0, \omega_2=0} = \frac{1}{1 + 4b_0 b_2 \omega_1^2}. \quad (16) \end{aligned}$$

Then  $ZCR_{\dot{r}}$  in (8) can be written as shown in (17) at the bottom of the next page. The above integral can be expanded as shown in

(18) at the bottom of the page, where  $g = 2b_2^2\omega_2^2(81 + 16b_2^2\omega_2^2)$ ,  $s = 1 + 18b_2^2\omega_2^2$ ,  $u = 64b_2^6\omega_2^6$ . Now, using the Residual Theorem in complex analysis, we have

$$\int_{-\infty}^{\infty} \frac{9(x^2 + 1) + g}{[(x^2 + s)^2 + u](x^2 + 1)} dx = 2\pi j \left\{ \frac{9 + \frac{g}{z_1^2 + 1}}{4\sqrt{u}jz_1} - \frac{9 + \frac{g}{z_2^2 + 1}}{4\sqrt{u}jz_2} + \frac{g}{2[(s-1)^2 + u]z_3} \right\} \quad (19)$$

where  $z_1 = (s^2 + u)^{1/4}(\cos(\theta/2) + j\sin(\theta/2))$ ,  $z_2 = (s^2 + u)^{1/4}(-\cos(\theta/2) + j\sin(\theta/2))$ , and  $z_3 = j$  are all three isolated singular points of the complex function

$$g(z) \equiv \frac{9(z^2 + 1) + g}{[(z^2 + s)^2 + u](z^2 + 1)}$$

in the upper half of the complex plane, and  $\theta$  satisfies  $\tan \theta = -\sqrt{u}/s$ . Substituting the results of (19) into (18), we obtain (20), shown at the bottom of the page.

Changing the variable  $t = b_2\omega_2$  in the integrand of (20), we have

$$\begin{aligned} \text{ZCR}_{\dot{r}} &= \frac{1}{4\pi} \sqrt{\frac{b_2}{b_0}} \\ &\times \int_{-\infty}^{\infty} \frac{1}{t^2} \left[ 1 - \frac{1}{\sqrt{2}} \frac{\sqrt{\sqrt{(1 + 18t^2)^2 + 64t^6} + 1 + 18t^2}}{\sqrt{(1 + 18t^2)^2 + 64t^6}} \right] dt. \end{aligned} \quad (21)$$

Numerical integration of the integral in (21) over all  $t$  yields 4.2757. Substituting  $b_0$  and  $b_2$  in (21) and simplifying, we obtain

$$\frac{1}{\text{ZCR}_{\dot{r}}} = \frac{4}{\sqrt{2} \times 4.2757 \times f_d} = \frac{0.6615}{f_d}. \quad (22)$$

By combining (6) and (22), we obtain an estimate of  $f_d$  as

$$\hat{f}_d \approx \frac{0.3308}{L_e \tau} \quad (23)$$

where  $L_e$  is the estimated AFSD from observations. Let  $N$  denote the number of sampling intervals in a positive (or negative) slope, and  $p(N = i)$  be the probability mass function (pmf) of  $N$  in our observation. The estimated AFSD can be computed as

$$L_e = \sum_i i \cdot p(N = i). \quad (24)$$

In the next section, we will show that it is sufficient to sum  $i$  from 1 to 20.

#### IV. SIMULATION RESULTS

The Rayleigh fading envelope is simulated using the simulator in [5], with a carrier frequency of 2 GHz and a sampling interval of  $\tau = 0.625$  ms. Fig. 2 shows the simulated probability mass function (pmf) of AFSD when the mobile velocities are 30, 60, and 90 km/h. The pmf is obtained by observing 1600 sampling intervals, which correspond to 1 s. The ideal value and the estimated value of AFSD are denoted by  $L^*$  and  $L_e$ , respectively. It is observed that the estimation error is within 3%.

The results of AFSD are used to estimate the mobile speed. The histograms of the velocity estimates for the true velocities at 20, 50, 90, and 120 km/h are plotted in Fig. 3, where  $v^*$  and  $v_e$  denote, respectively, the true and estimated velocities. The standard deviation

$$\text{std} = \sqrt{(v^* - v_e)^2}$$

is within 2.4 km/h. The estimation errors, denoted as normalized square error (NSE) =  $(1 - v_e/v^*)^2$ , are  $1.4e-3$ ,  $1.4e-3$ ,  $1.04e-4$ , and  $2.9e-5$  for velocity changes from 20 to 120 km/h,

$$\text{ZCR}_{\dot{r}} = \frac{-1}{2\pi^2} \int_{-\infty}^{\infty} \int_{-\infty}^{\infty} \frac{-18b_2^2 + 8jb_2^3\omega_2}{(1 + 4b_0b_2\omega_1^2 + 18b_2^2\omega_2^2 - 8jb_2^3\omega_2^3)(1 + 4b_0b_2\omega_1^2)} d\omega_1 d\omega_2 \quad (17)$$

$$\begin{aligned} \text{ZCR}_{\dot{r}} &= \frac{b_2^2}{\pi^2} \int_{-\infty}^{\infty} \int_{-\infty}^{\infty} \frac{9(1 + 4b_0b_2\omega_1^2) + 2b_2^2\omega_2^2(81 + 16b_2^2\omega_2^2)}{[(1 + 4b_0b_2\omega_1^2 + 18b_2^2\omega_2^2)^2 + 64b_2^6\omega_2^6](1 + 4b_0b_2\omega_1^2)} d\omega_1 d\omega_2 \\ &- \frac{4b_2^3}{\pi^2} j \int_{-\infty}^{\infty} \int_{-\infty}^{\infty} \frac{\omega_2}{(1 + 4b_0b_2\omega_1^2 + 18b_2^2\omega_2^2)^2 + 64b_2^6\omega_2^6} d\omega_1 d\omega_2 = \frac{b_2^2}{2\sqrt{b_0b_2}\pi^2} \int_{-\infty}^{\infty} \int_{-\infty}^{\infty} \frac{9(x^2 + 1) + g}{[(x^2 + s)^2 + u](x^2 + 1)} dx d\omega_2 \end{aligned} \quad (18)$$

$$\begin{aligned} \text{ZCR}_{\dot{r}} &= \frac{b_2^2}{2\sqrt{b_0b_2}\pi^2} \int_{-\infty}^{\infty} \frac{\pi}{2b_2^2\omega_2^2} \left( 1 - \frac{1}{(s^2 + u)^{1/4}} \sin \frac{\theta}{2} \right) d\omega_2 = \frac{1}{4\sqrt{b_0b_2}\pi} \int_{-\infty}^{\infty} \frac{1}{\omega_2^2} \left( 1 - \frac{1}{(s^2 + u)^{1/4}} \sin \frac{\theta}{2} \right) d\omega_2 \\ &= \frac{1}{4\sqrt{b_0b_2}\pi} \int_{-\infty}^{\infty} \frac{1}{\omega_2^2} \left( 1 - \frac{1}{\sqrt{2}} \frac{\sqrt{\sqrt{s^2 + u} + s}}{\sqrt{s^2 + u}} \right) d\omega_2 \\ &= \frac{1}{4\sqrt{b_0b_2}\pi} \int_{-\infty}^{\infty} \frac{1}{\omega_2^2} \left( 1 - \frac{1}{\sqrt{2}} \frac{\sqrt{\sqrt{(1 + 18b_2^2\omega_2^2)^2 + 64b_2^6\omega_2^6} + 1 + 18b_2^2\omega_2^2}}{\sqrt{(1 + 18b_2^2\omega_2^2)^2 + 64b_2^6\omega_2^6}} \right) d\omega_2 \end{aligned} \quad (20)$$

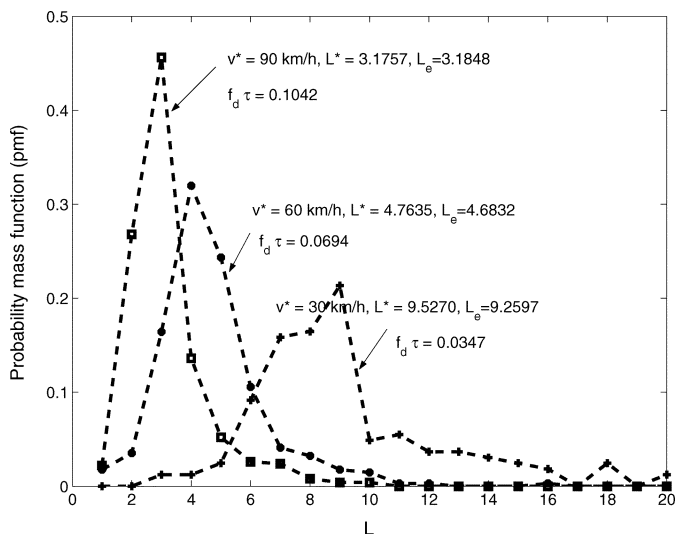


Fig. 2. Discrete pmf of the observations for parameter  $L$ .

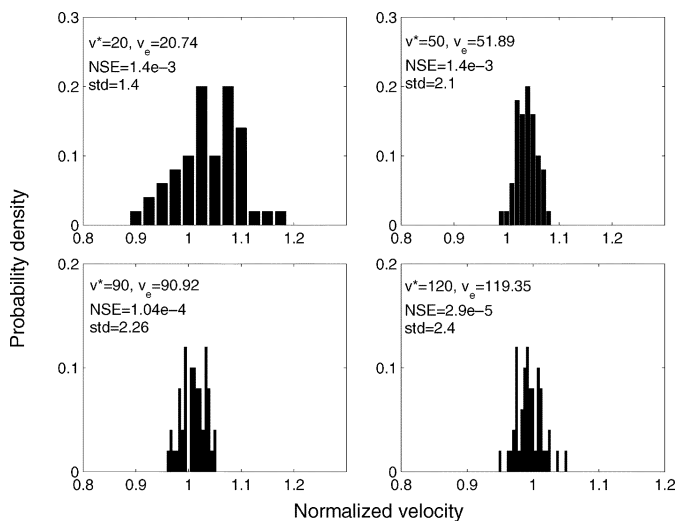


Fig. 3. Histogram of the velocity estimates.

respectively. Comparing our NSE numbers with the results presented in [4, Fig. 5], where the best NSE number is close to  $4e - 3$ , the AFSD scheme exhibits a lower NSE, and therefore offers better accuracy, compared with the CWT scheme.

For speed-estimation schemes reported in the literature where the observation window is required, computation can only be carried out after all the samples have been obtained. However, the AFSD approach can process the data when the sampling process is ongoing. It only needs a very limited number of samples to obtain the estimate; therefore, the proposed scheme is quite efficient in terms of computational complexity and memory storage requirement.

With the proposed AFSD scheme, we can obtain  $2L$  effective samples for processing without increasing the sampling rate, whereas other schemes which employ either LCR or ZCR for speed estimation only obtain one sample per acquisition period. Thus, the proposed AFSD approach uses less time to accomplish accurate speed estimation.

Although it has not been explicitly shown in the text, the proposed AFSD-based estimation scheme also works in a noisy environment. At low signal-to-noise ratios, the accuracy improves with speed. Thus, the proposed estimation scheme is particularly suited for high mobile speed estimation.

### V. CONCLUDING REMARKS

We have proposed a new mobile speed-estimation scheme based on counting and averaging the number of sampling steps in a fading envelope slope. Germane to the derivation of the mobile speed-estimation scheme is the introduction of the AFSD and the establishment of a relationship between AFSD and the ZCR of the slope of the Rayleigh fading envelope. The derivation of the ZCR of envelope slope can also be generalized to a Rician fading envelope.

Simulation results show that, compared to the CWT approach, the proposed scheme exhibits better velocity estimates with relatively smaller estimation error and a lower computation effort.

With a simple implementation feature and good estimation accuracy, the proposed mobile speed-estimation approach can be used to design effective closed-loop power control and handoff strategies.

### REFERENCES

- [1] M. D. Austin and G. L. Stüber, "Velocity adaptive handoff algorithms for microcellular systems," *IEEE Trans. Veh. Technol.*, vol. 43, pp. 549–561, Aug. 1994.
- [2] J. M. Holtzman and A. Sampath, "Adaptive averaging methodology for handoffs in cellular systems," *IEEE Trans. Veh. Technol.*, vol. 44, pp. 59–66, Feb. 1995.
- [3] K. D. Anim-Appiah, "On generalized covariance-based velocity estimation," *IEEE Trans. Veh. Technol.*, vol. 48, pp. 1546–1557, Sept. 1999.
- [4] R. Narasimhan and C. Cox, "Speed estimation in wireless systems using wavelets," *IEEE Trans. Commun.*, vol. 47, pp. 1357–1364, Sept. 1999.
- [5] W. C. Jakes, *Microwave Mobile Communications*. New York: Wiley, 1993.
- [6] G. L. Stüber, *Principles of Mobile Communications*, 2nd ed. Norwell, MA: Kluwer, 2001.
- [7] A. Abdi and M. Kaveh, "Level crossing rate in terms of the characteristic function: A new approach for calculating the fading rate in diversity systems," *IEEE Trans. Commun.*, vol. 50, pp. 1397–1400, Sept. 2002.
- [8] G. L. Turin, "The characteristic function of Hermitian quadratic forms in complex normal variables," *Biometrika*, vol. 47, pp. 199–201, 1960.